Science and Technology Indonesia
e-ISSN:2580-4391 *p*-ISSN:2580-4405
Vol. 10, No. 2, April 2025

Research Paper

Stability and Antiaging Effectiveness Studies of Astaxanthin-Loaded Nanostructured Lipid Carriers Using a Combination of Cetyl Palmitate and Soybean Oil

Dzakiya Zhihrotulwida[1,5], Widji Soeratri[2,3], Tristiana Erawati[2,3,4], Noorma Rosita[2,3,4*]

[1]*Master's Program in Pharmaceutical Sciences, Faculty of Pharmacy, Universitas Airlangga, Surabaya, 60115, Indonesia*
[2]*Department of Pharmaceutical Sciences, Faculty of Pharmacy, Universitas Airlangga, Surabaya, 60115, Indonesia*
[3]*Skin and Cosmetic Technology (SCT) Centre of Excellent, Universitas Airlangga, Surabaya, 60115, Indonesia*
[4]*Pharmaceutics and Delivery Systems for Drugs, Cosmestics, and Nanomedicine Research Group, Universitas Airlangga Surabaya, 60115, Indonesia*
[5]*Department of Pharmacy, Universitas Anwar Medika, Sidoarjo, 61262, Indonesia*
***Corresponding author**: noorma-r@ff.unair.ac.id

Abstract
Astaxanthin is a potent antioxidant belonging to carotenoid compounds that is mainly produced from green microalgae *Haematococcus pluvialis*. Astaxanthin is beneficial for skin health as antiaging agent, but has limitations in its delivery through the skin. Astaxanthin could be formulated in nanostructured lipid carriers to improve its efficacy. The purpose of this study was to evaluate the stability and antiaging effectiveness of astaxanthin-loaded nanostructured lipid carriers (ASX-NLCs) with cetyl palmitate and soybean oil as lipid combinations at several ratios of 100:0, 90:10, 80:20, and 70:30. ASX-NLCs were synthesized using a high-shear homogenization technique. ASX-NLCs were characterized and stability evaluated after storage for 90 days. The antiaging effectiveness of ASX-NLCs was evaluated by in vitro release test using dialysis bag for 8 hours, as well as collagen density and fibroblast count evaluation on UV-induced skin aging mice for 28 days. After storage, all ASX-NLCs did not change significantly in organoleptic, pH, and particle size. However, other parameters including polydispersity index, viscosity, and entrapment efficiency experienced significant changes in some formulas. The release test showed that F4 (70:30) gave the highest cumulative release and was significantly different from F1 (100:0). The collagen density of the groups treated with ASX-NLC F3 (80:20) and F4 (70:30) increased significantly compared to the UVB control group, while the fibroblast count did not differ significantly in all groups. Overall, ASX-NLCs containing cetyl palmitate and soybean oil at ratios of 80:20 and 70:30 could improve the antiaging effect of astaxanthin which might be influenced by its better stability and release.

Keywords
Nanostructured Lipid Carriers, Astaxanthin, Cetyl Palmitate, Soybean Oil, Antiaging

Received: 8 November 2024, Accepted: 8 February 2025
https://doi.org/10.26554/sti.2025.10.2.473-481

1. INTRODUCTION

Skin aging is a complex biological process of cumulative changes in the structure, function, and appearance of the skin which is influenced by various factors, both intrinsic and extrinsic factors. As people age, the epidermis becomes thinner and the dermal-epidermal junction becomes flattened. In addition, fibroblasts undergo structure and morphology changes that lead to a decrease in collagen and elastin synthesis. As a result, skin resilience is reduced which clinically manifests as sagging and wrinkling of the skin (Lee et al., 2021). Exposure to ultraviolet (UV) rays can accelerate skin aging by elevating the expression of matrix metalloproteinase genes, thereby enhancing the degradation of collagen and elastin. About 80% of facial skin aging occurs due to UV exposure (Zhang and Duan, 2018). Antiaging cosmetics containing powerful antioxidants are widely used to prevent and reduce clinical signs of skin aging, astaxanthin is one of them.

Astaxanthin is a xanthophyll carotenoid compound which can be found in various microorganisms and marine animals as a red-orange pigment. For human consumption, astaxanthin is mainly produced from green microalgae *Haematococcus pluvialis*. Topical application of astaxanthin is known to be beneficial for skin health. As antiaging, astaxanthin can inhibit cell damage caused by free radicals and UV radiation (Davinelli et al., 2018). Astaxanthin can also increase fibroblasts viability and increase collagen levels by inhibiting matrix metalloproteinase (MMP) expression in fibroblasts (Chou et al., 2016). However, topical application of astaxanthin has some limitations. Its large molecular weight (596.85 g/mol) and highly lipophilic nature (logP

of 13.27) makes it difficult for astaxanthin to permeate into the dermis layer to provide antiaging effects (Lima et al., 2021; Souto et al., 2022). In addition, astaxanthin is susceptible to degradation due to the presence of conjugated polyene chain which is characteristic of carotenoid compounds (Dewati et al., 2022).

The development of nanostructured lipid carriers (NLCs) formulations, which is one of the lipid-based drug delivery systems, is promising to enhance the stability and penetration of the active ingredients into the skin, especially for lipophilic compounds such as astaxanthin. NLCs are lipid nanoparticles that use a combination of solid lipids and liquid lipids as lipid matrix components and are stabilized by surfactants. Lipid is the main component of NLC which affect the loading capacity and release action of active substance, as well as the stability of the formulation (Chauhan et al., 2020).

Several studies on astaxanthin-loaded NLCs (ASX-NLCs) using various lipid combinations have been conducted with focusing on formula development and evaluating the effect of formula composition on NLC particle characteristics. Formula composition, such as the liquid lipid content in the lipid matrix, has a significant effect on its physical characteristics and storage stability (Tamjidi et al., 2014). Rodriguez-Ruiz et al. (2018) studied that NLC formulation is able to maintain the antioxidant activity of astaxanthin. Geng et al. (2020) reported in vitro skin permeation and skin retention studies showing that ASX-NLC was able to permeate into the skin with better skin retention without damaging the skin. These results suggested that NLC can be a promising astaxanthin carrier (Geng et al., 2020). The effectiveness of ASX-NLC as an antiaging agent on the skin has not been studied in previous studies, especially regarding its effect in increasing collagen density and fibroblast count in the skin. Therefore, this study focuses on evaluating the stability and antiaging effectiveness of ASX-NLCs.

A combination of solid lipid cetyl palmitate and liquid lipid soybean oil was used in this study. Sensitive active substances, such as astaxanthin, can be protected by the physical barrier properties of cetyl palmitate (Putranti et al., 2017). Using vegetable oil, such as soybean oil, in NLC formulations can help protect astaxanthin from oxidation due to its natural antioxidant content (Rodriguez-Ruiz et al., 2018). The ASX-NLCs were prepared in this study with several ratios of cetyl palmitate and soybean oil ranging from 100:0 to 70:30. This study was designed to evaluate the stability and antiaging effectiveness of ASX-NLCs containing a mixture of solid lipid cetyl palmitate and liquid lipid soybean oil as lipid matrix components at several ratios.

2. EXPERIMENTAL SECTION

2.1 Materials

The following materials were used in this study including astaxanthin oleoresin 5% (AstaLuxe^{TM}, PT. Evergen Resources, Indonesia), cetyl palmitate (BASF, Germany), soybean oil (CV. INBI Nusantara, Indonesia), Tween 80 (KAO Corporation, Japan), Span 80 (Croda Singapore Pte. Ltd.), propylene glycol (Dow Chemical Pacific Pte. Ltd. Singapore), Nipaguard SCP (Clariant International Ltd. Switzerland), sodium dihydrogen phosphate and disodium hydrogen phosphate (Merck, Germany), ethanol for analysis, and sodium lauryl sulfate.

2.2 Astaxanthin-Loaded NLC Preparation

Four formulas of ASX-NLC were prepared using a high-shear homogenization technique with different ratios of solid lipid cetyl palmitate and liquid lipid soybean oil, namely 100:0 (F1), 90:10 (F2), 80:20 (F3), and 70:30 (F4). The formulas can be seen in Table 1. The formulas contain astaxanthin oleoresin as active ingredient, combination of solid lipid cetyl palmitate and liquid lipid soybean oil as lipid matrix components, Tween 80 and Span 80 as surfactants, propylene glycol as cosurfactant, Nipaguard SCP as preservative, and distilled water as water phase. The oil phase components including cetyl palmitate, soybean oil, Span 80, and astaxanthin oleoresin were mixed and heated at 65 °C. Meanwhile, the aqueous phase components including Tween 80, propylene glycol, and distilled water were mixed in different container and heated at 65 °C. Then the aqueous phase was poured into the oil phase slowly and stirred using a T25 digital ULTRA-TURRAX®Homogenizer (IKA-Werke GmbH & Co. KG, Germany) at a speed of 5,000 rpm for 5 minutes in 3 cycles while still heated at 65 °C. Then stirred again at 17,000 rpm for 3 minutes in 3 cycles. After that, the heating process was stopped and Nipaguard SCP was added into the preparation. Then the preparation was cooled down to room temperature while being stirred using a magnetic stirrer at 700 rpm.

2.3 Astaxanthin-Loaded NLC Characterization

The ASX-NLC was characterized by evaluating particle size, polydispersity index, particle morphology, and entrapment efficiency. Particle size and polydispersity index were measured using a DelsaTM Nano C Particle Size Analyzer (Beckman Coulter Inc., USA). The measurements were carried out in triplicate. Particle morphology was observed using a Hitachi FlexSEM Scanning Electron Microscope (Hitachi High-Technologies Corporation, Japan). The entrapment efficiency of ASX-NLC was determined by centrifuging ASX-NLC sample (1 g) for 90 minutes at 15,000 rpm and 4 °C using a BOECO Centrifuges M-240R (Boeckel & Co. GmbH & Co. KG, Germany). The supernatant from centrifugation (contained free astaxanthin) was collected and diluted in ethanol (1:100), then measured at a wavelength of 474.6 nm using a Hitachi UH5300 UV-visible spectrophotometer (Hitachi High-Technologies Corporation, Japan). After that, the entrapment efficiency was calculated using the following Equation (1):

$$\text{Entrapment Efficiency (\%)} = \left(\frac{W_{\text{total ASX}} - W_{\text{free ASX}}}{W_{\text{total ASX}}}\right) \times 100\% \quad (1)$$

Table 1. Four Formulas of ASX-NLC

Ingredient	Concentration (%, w/w)			
	F1	F2	F3	F4
Astaxanthin oleoresin	0.07	0.07	0.07	0.07
Cetyl palmitate	5	4.5	4	3.5
Soybean oil	-	0.5	1	1.5
Tween 80	8.97	8.97	8.97	8.97
Span 80	11.03	11.03	11.03	11.03
Propylene glycol	10	10	10	10
Nipaguard SCP	0.5	0.5	0.5	0.5
Distilled water	64.43	64.43	64.43	64.43

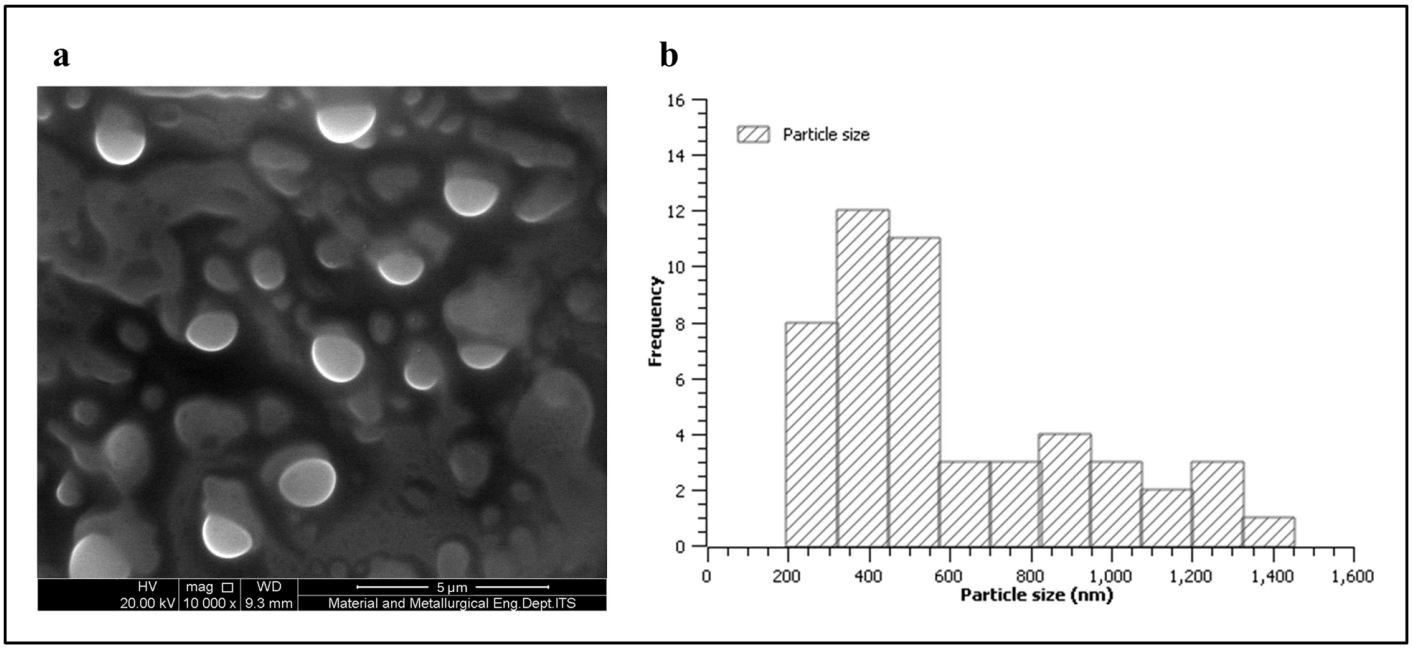

Figure 1. (a) SEM Image of ASX-NLC F4 (10,000× Magnification) and (b) Histogram of Particle Size Distribution Determined From the SEM Image

Where, $W_{\text{total ASX}}$ is the total amount of astaxanthin used in the formula and $W_{\text{free ASX}}$ is the amount of free astaxanthin in the supernatant (Patil et al., 2016). The measurement was carried out in triplicate.

2.4 Stability Study

The stability test was performed by storing the ASX-NLCs for 90 days at room temperature (25 ± 2 °C), in a tightly closed container and protected from light (Erawati et al., 2023). The stability parameters evaluated were organoleptic, pH (Eutech™ pH 700, Eutech Instruments Pte. Ltd., Singapore), particle size, polydispersity index, viscosity using a CP-51 spindle at a speed of 100 rpm (Brookfield DV-I+ Viscometer, Brookfield Engineering Laboratories Inc., USA), and entrapment efficiency. Each measurement was carried out in triplicate.

2.5 Antiaging Effectiveness Study

2.5.1 In Vitro Release Test

In vitro release test was performed using the dialysis bag method. The ASX-NLC sample (3 g) was placed in a dialysis bag (molecular weight cut-off 10,000–14,000 Da), then placed into a mixture of phosphate buffer solution and 1% sodium lauryl sulphate (60 mL, pH 6.00 ± 0.05). During the test, the media was stirred at a speed of 100 rpm and the temperature was maintained at 32 ± 0.5 °C (Olejnik et al., 2012; Tichý et al., 2011). A total of 3 mL of sample was taken from the receptor media at predetermined time intervals (10, 20, 30, 60, 90, 120, 180, 240, 300, 360, 420, and 480 minutes). To maintain sink conditions, the removed media was replaced with a same volume of fresh media. The samples were analyzed at a wavelength of 482.8 nm using a Hitachi UH5300 UV-visible spectrophotometer. The cumulative release percentages of

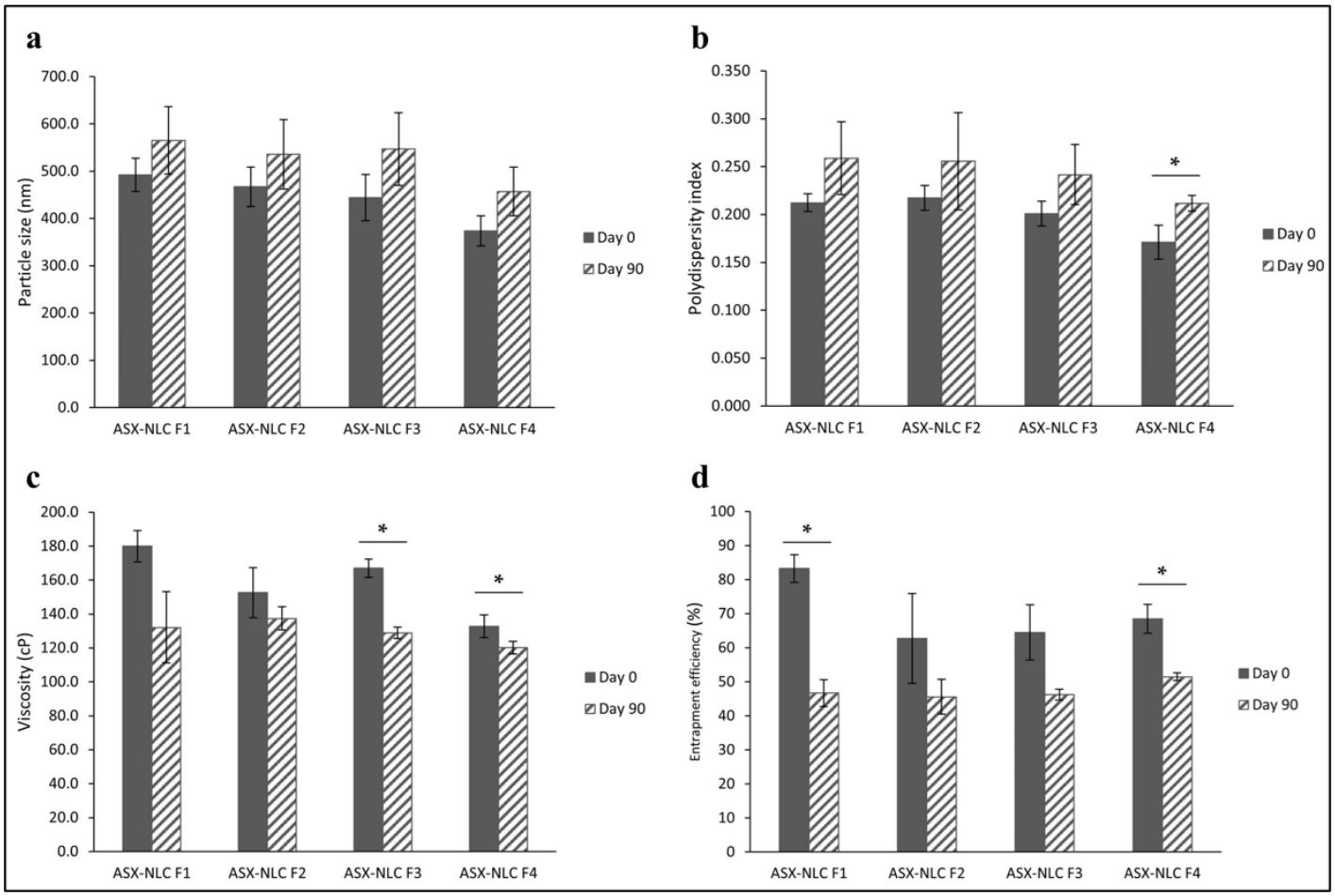

Figure 2. The Graphs Represent the Stability Study of ASX-NLCs After Storage for 90 Days at Room Temperature with Parameters Including (a) Particle Size, (b) Polydispersity Index, (c) Viscosity, and (d) Entrapment Efficiency (* p <0.05)

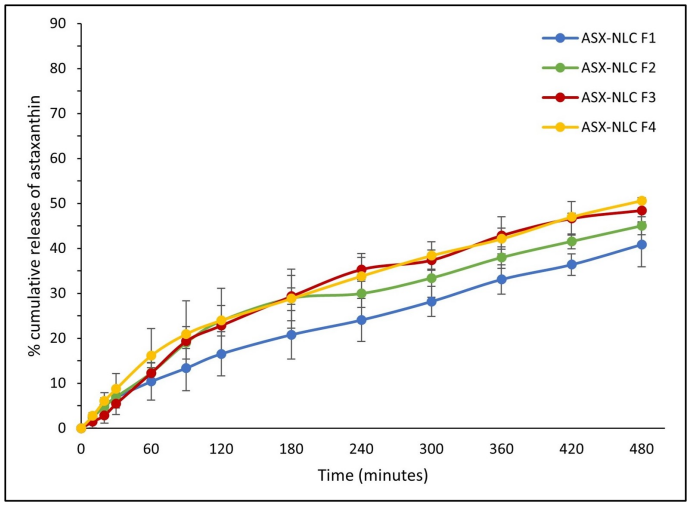

Figure 3. In Vitro Release Profiles of Astaxanthin from ASX-NLCs F1, F2, F3, and F4

astaxanthin were calculated and plotted against time.

2.5.2 Evaluation of Collagen Density and Fibroblast Count

The collagen density and fibroblast count evaluation was carried out on mice (*Mus musculus*) with UV-induced skin aging. This work was performed after obtaining ethical clearance from Health Research Ethical Clearance Commission of the Faculty of Dental Medicine, Universitas Airlangga with number 1302/HRECC.FODM/XII/2023.

A total of 24 male mice aged 6–8 weeks (weighing 20–30 g) were divided into six groups as follows: 1) group treated with UVB irradiation and ASX-NLC F1, 2) group treated with UVB irradiation and ASX-NLC F2, 3) group treated with UVB irradiation and ASX-NLC F3, 4) group treated with UVB irradiation and ASX-NLC F4, 5) group given UVB irradiation without ASX-NLC (UVB control), and 6) group not given both UVB irradiation and ASX-NLC (normal control). All mice had their backs shaved (2 × 2 cm) before the ASX-NLC was applied. Each ASX-NLC according to the treatment was applied twice daily on the shaved dorsal skin of mice at 50 μL/cm^2 of skin area, 20 minutes before UVB irradiation (to

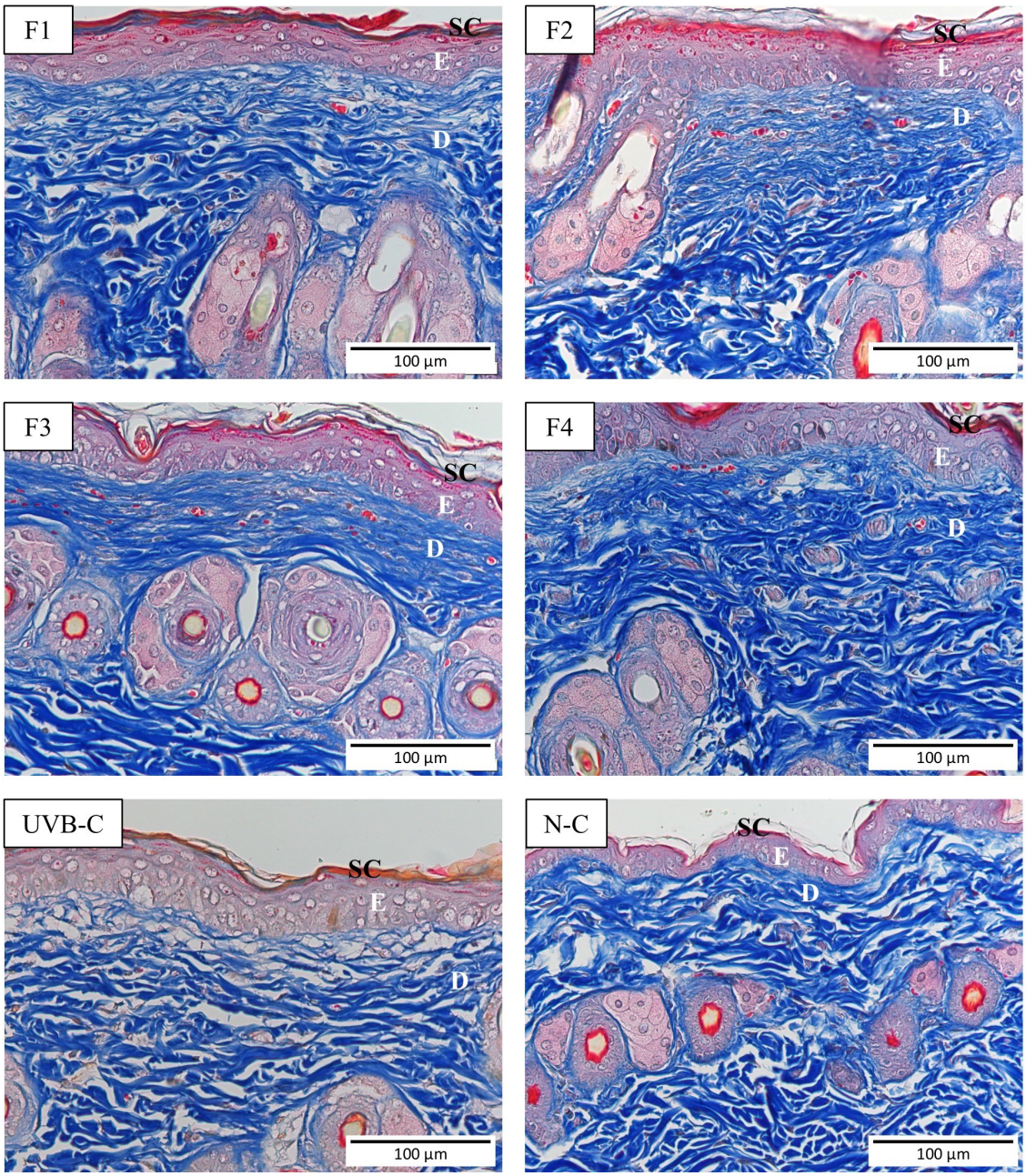

Figure 4. Photomicrographs of Collagen Density (Blue Color in the Dermis Layer) With Mallory Azan Staining from the ASX-NLC F1–F4 Treatment Groups, UVB Control (UVB-C) Group, and Normal Control (N−C) Group. SC = Stratum Corneum, E = Epidermis, and D = Dermis

provide time for topical absorption) and 4 hours after UVB irradiation (reactive oxygen species formation begins at 4 hours after exposure). UVB irradiation was carried out every two days with an intensity of 80 mJ/cm^2 for 34 minutes. The application of ASX-NLC was still carried out on days without UVB irradiation (Apsari et al., 2020; Miatmoko et al., 2022).

After 28 days, the mice were sacrificed. Skin tissue samples were collected from the application area and soaked in 10% Neutral Buffered Formalin (NBF) solution for making histopathological preparations of skin tissue. Then the tissue preparations were stained with Mallory Azan to observe the collagen density and hematoxylin-eosin to observe the fibroblast count. The skin tissue preparations were observed under a light microscope. The collagen density was analyzed using ImageJ software and the fibroblast count was determined manually (Miatmoko et al., 2022).

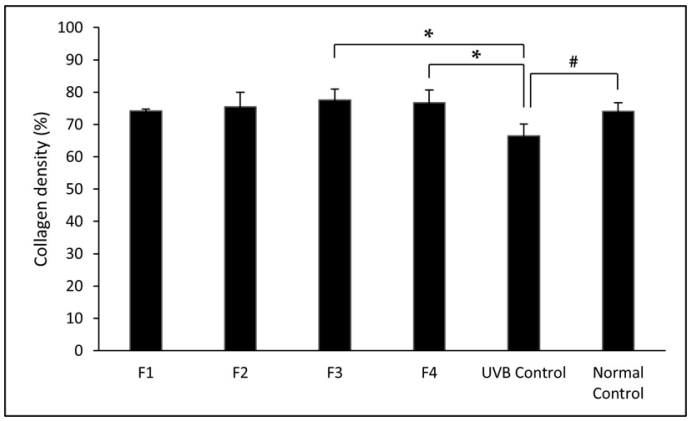

Figure 5. Graph Representing Collagen Density in the Groups Treated With ASX-NLC F1, F2, F3, and F4, as Well as the UVB Control and Normal Control Groups (* p ± 0.05 based on the Tukey HSD Post Hoc Test, # p ± 0.05 Based on Independent-Samples T-test)

2.6 Statistical Analysis

Data were presented as mean ± standard deviation (SD). A paired-samples t-test was performed to analyze the data before and after storage in the stability study. To determine the significant differences between groups in antiaging effectiveness study, multiple comparisons were performed using a one-way analysis of variance (ANOVA) with Tukey HSD post hoc test. The UVB control and normal control groups in the antiaging effectiveness study were compared statistically using an independent-samples t-test. Data was considered statistically significant if the p-value <0.05.

3. RESULTS AND DISCUSSION

3.1 Astaxanthin-Loaded NLC Characterization

The ASX-NLCs with four different formulas were successfully prepared. Each ASX-NLC from F1 to F4 had a particle size of 491.8 ± 35.1 nm, 466.8 ± 41.8 nm, 444.0 ± 48.8 nm, and 373.8 ± 31.8 nm, respectively. All ASX-NLCs of the four formulas had homogeneous particle size distributions with polydispersity index ranging from 0.171 ± 0.018 to 0.217 ± 0.013.

The ASX-NLC with smallest particle size (F4) was observed for particle morphology using a Scanning Electron Microscope (SEM) at 10,000× magnification. The ASX-NLC appeared spherical in shape with a smooth surface as shown in Figure 1a. This is in line with other studies that reported that lipid nanoparticles appeared spherical and had smooth surface (Hariyadi et al., 2024). The size distribution of ASX-NLCs particles measured from the SEM image can be seen in Figure 1b. The average particle size measured from the SEM image was 608.1 nm, different from the average particle size measured using a particle size analyzer. Some particles in the SEM image appeared larger. The accuracy of measurement results using the tool was more valid compared to manual measurement (Mardiyanto et al., 2021).

The entrapment efficiency was calculated for each ASX-NLC to determine the efficiency of the nanoparticles in entrapping astaxanthin in a lipid matrix consisting of the solid lipid cetyl palmitate and the liquid lipid soybean oil in several ratios. Each ASX-NLC formula from F1 to F4 was able to produce lipid nanoparticles that efficiently trapped astaxanthin with entrapment efficiency values of 83.25 ± 4.10%, 62.73 ± 13.22%, 64.51 ± 8.15%, and 68.52 ± 4.21%, respectively.

3.2 Stability Study

The ASX-NLCs were observed organoleptically on day 0 and 90. All ASX-NLCs appeared orange in color with a slightly thick liquid consistency. No phase separation was observed in any ASX-NLC. After 90 days of storage, all ASX-NLCs showed no visual changes and no phase separation.

Freshly prepared ASX-NLCs from F1 to F4 had pH values of 6.68 ± 0.02, 6.75 ± 0.01, 6.65 ± 0.08, and 6.62 ± 0.08, respectively. The pH values of ASX-NLCs showed slight increase after 90 days of storage with a pH range being 6.62 ± 0.08 to 6.84 ± 0.08. The pH measurement results demonstrated that the ASX-NLC formulas are suitable for topical application according to the normal skin pH range of 4.0–7.0 (Lambers et al., 2006).

Particle size and polydispersity index tended to increase in all ASX-NLCs after 90 days of storage (Figures 2a and 2b). The particle sizes of ASX-NLCs F1–F4 increased by 14.89%, 14.72%, 23.11%, and 22.26%, respectively. However, the increase in particle size in each ASX-NLC was not statistically significant. The polydispersity index of ASX-NLC F1–F4 increased by 22.17%, 17.97%, 20.40%, and 23.98% respectively, with a significant increase in ASX-NLC F4. However, the particle size distributions of all ASX-NLCs were still homogenous after 90 days of storage (polydispersity index <0.3).

Each ASX-NLC from F1 to F4 had a viscosity of 179.9 ± 9.2 cP, 152.6 ± 14.8 cP, 166.9 ± 5.5 cP, and 132.8 ± 6.7 cP. Increasing the amount of liquid lipid in the nanoparticle formulation decreased the viscosity of the system (Erawati et al., 2021). The viscosity of all ASX-NLCs tended to decrease after 90 days of storage (Figure 2c), with significant decreases in F3 (128.9 ± 3.4 cP) and F4 (120.1 ± 3.7 cP). After storage, the formulas with more liquid lipids (F3 and F4) were less stable in viscosity.

After 90 days of storage, the entrapment efficiency of all ASX-NLCs also tended to decrease, with significant decreases in F1 and F4 (Figure 2d). The entrapment efficiency of ASX-NLC F1 decreased by 36.57% and ASX-NLC F4 decreased by 17.08% from the initial value. This showed that ASX-NLC F1 experienced greater drug expulsion during storage compared to other formulas. During the cooling process in the lipid nanoparticles manufacture, the droplets recrystallize in the higher energy α and β modifications. These modifications are relatively unstable. During storage, these modifications transform to the lower energy and more ordered β modification (Punu et al., 2023). The lipid matrix of ASX-NLC F1 was

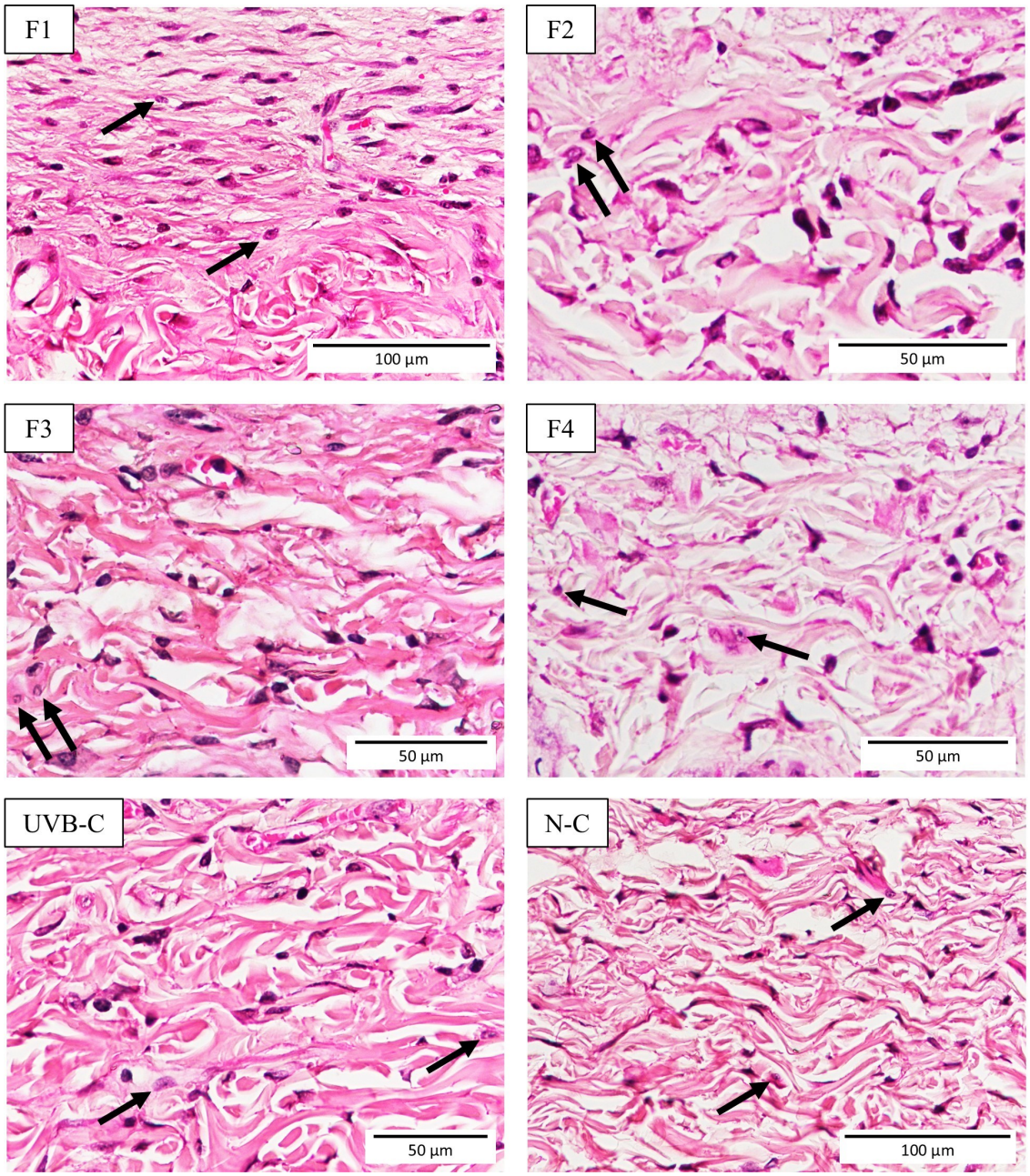

Figure 6. Photomicrographs of Fibroblasts in the Dermis Layer with Hematoxylin-eosin Staining from the ASX-NLC F1–F4 Treatment Groups, UVB Control (UVB-C) Group, and Normal Control (N-C) Group. Black Arrows Show Young Fibroblasts

composed of cetyl palmitate without soybean oil. The lipid matrix consisting only of solid lipid with a highly ordered crystal lattice arrangement was more susceptible to drug expulsion due to polymorphic transition of solid lipid crystals during storage, thereby reducing the entrapment efficiency.

3.3 Antiaging Effectiveness Study

3.3.1 In Vitro Release Test

The in vitro astaxanthin release profiles from ASX-NLCs F1–F4 for 8 hours were shown in Figure 3. The cumulative release percentages of astaxanthin from ASX-NLC F1 to F4 were 40.87 ± 4.99%, 45.00 ± 1.99%, 48.45 ± 2.80%, and 50.63 ± 0.05%, respectively. The total amount of release after 8 hours increased from F1 to F4, as the soybean oil content increased. ASX-NLC F4 (70:30) provided the highest cumulative release percentage and was significantly different from ASX-NLC F1 (100:0).

The release of encapsulated substance can be influenced by various factors. Smaller particles may have faster release due to larger surface area and shorter diffusion paths compared

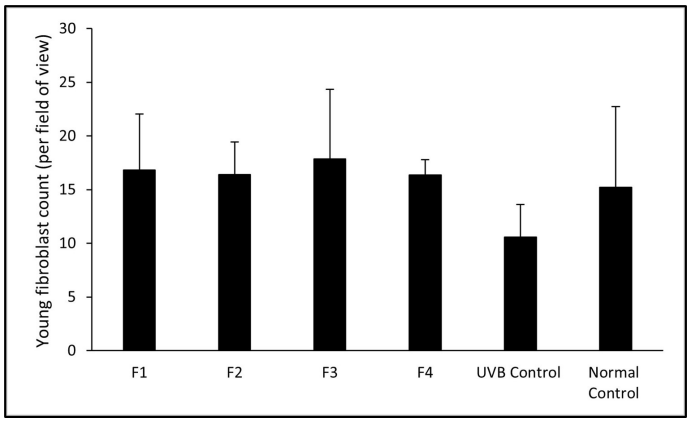

Figure 7. Graph Representing the Young Fibroblast Count in the Groups Treated with ASX-NLC F1, F2, F3, and F4, as Well as the UVB Control and Normal Control Groups

to larger particles (Khosa et al., 2018). In this study, increasing soybean oil in the ASX-NLC formula tended to produce smaller particle sizes, but the particle sizes of all formulas did not differ significantly based on one-way ANOVA ($p < 0.05$). The viscosity of lipid nanoparticles may be another explanation. Nanoparticles with a solid lipid matrix have a higher viscosity which makes particle movement more difficult, thus slowing down the active substance release. By adding soybean oil, the viscosity of the lipid nanoparticle matrix is reduced, resulting in faster diffusion (Erawati et al., 2021).

3.3.2 Evaluation of Collagen Density and Fibroblast Count

Collagen density was evaluated through histopathological analysis with Mallory Azan staining. Photomicrographs of collagen density observation were shown in Figure 4. Collagen fibers were characterized by blue color. Each group treated with ASX-NLC F1–F4 had a collagen density of 74.14 ± 0.60%, 75.52 ± 4.46%, 77.58 ± 3.31%, and 76.65 ± 4.00%, while the UVB control group and the normal control group had a collagen density of 66.42 ± 3.68% and 74.08 ± 2.67%, respectively (Figure 5). UVB irradiation significantly reduced skin collagen density. Compared to the normal control group, the collagen density of the UVB control group was significantly lower. UVB exposure induced excessive expression of several matrix metalloproteinases (MMPs) in the skin, such as MMP 1, 3, and 9, resulting in collagen fragmentation (Kang et al., 2020). Meanwhile, the groups treated with ASX-NLC F3 and F4 presented significantly higher collagen density compared to the UVB control group. These results showed that topical application of ASX-NLC F3 and F4 was able to prevent photoaging.

Fibroblasts were observed by hematoxylin-eosin staining. Photomicrographs of fibroblasts in dermis layer were shown in Figure 6. Aged skin is characterized by a decrease in the number of young fibroblasts (Nanic et al., 2022). Therefore, young fibroblasts were counted for comparison between groups in this study. The count of young fibroblasts per field of view in each group treated with ASX-NLC F1–F4 was 16.83 ± 5.23, 16.43 ± 3.03, 17.88 ± 6.45, and 16.35 ± 1.44, respectively. While in the UVB control and normal control groups, it was 10.57 ± 3.05 and 15.22 ± 7.51 (Figure 7). All groups showed no statistically significant differences in young fibroblast count.

Increasing the soybean oil content in the ASX-NLC formula to a lipid ratio of 80:20 (F3) and 70:30 (F4) could improve the antiaging effect of ASX-NLC which was characterized by increased skin collagen density. The antiaging effect of ASX-NLCs might be related to its stability and release profile. The results of the stability evaluation indicated that the formula without soybean oil addition (F1) experienced a greater decrease in entrapment efficiency after storage compared to the formulas containing soybean oil as a component of the lipid matrix (F2–F4). Increasing the soybean oil content in the ASX-NLC formula reduced drug expulsion, resulting in more astaxanthin being protected in the lipid matrix during storage. Meanwhile, the results of in vitro release test showed that soybean oil addition in the ASX-NLC formula provided a faster release of astaxanthin with a significant increase at a solid lipid to liquid lipid ratio of 70:30 (F4). The good stability of ASX-NLC could maintain the astaxanthin content and ASX-NLC with a faster release profile could increase the amount of astaxanthin release from the lipid matrix, thus providing more astaxanthin to work on the target area of the skin and improving the antiaging effects.

4. CONCLUSIONS

In this study, ASX-NLCs containing a combination of solid lipid cetyl palmitate and liquid lipid soybean oil at a ratio between 100:0 to 70:30 tended to show good stability over 90 days of storage. However, there was a significant decrease in viscosity at the ratios of 80:20 and 70:30 after storage. In addition, ASX-NLC that did not contain soybean oil as a lipid matrix component experienced the greatest decreased in entrapment efficiency after storage. The release of astaxanthin from NLC system containing solid lipid cetyl palmitate and liquid lipid soybean oil at a ratio of 100:0 to 70:30 tended to increase by increasing the soybean oil content. The topical administration of ASX-NLCs containing cetyl palmitate and soybean oil at ratios of 80:20 and 70:30 was able to prevent photoaging, as indicated by increased collagen density. This study was limited to four different ratios of solid lipid cetyl palmitate and liquid lipid soybean oil. For further studies to determine the effect of the combination of solid lipid cetyl palmitate and liquid lipid soybean oil on the stability and effectiveness of ASX-NLC, more variations in the lipid ratio and other evaluation parameters may be needed.

5. ACKNOWLEDGEMENT

The authors would like to express their gratitude to the Directorate of Research, Technology, and Community Service, Directorate General of Higher Education, Research, and Technology (DRTPM Ditjen Diktiristek) of the Ministry of Edu-

cation, Culture, Research, and Technology of the Republic of Indonesia for its funding support through the Master's Thesis Research grant in 2024.

REFERENCES

Apsari, K. J. T., I. G. A. D. Ratnayanti, I. G. K. N. Arijana, and I. W. Sugiritama (2020). Topical Application of Purple Cabbage (*Brassica oleracea* L. var. *capitata* f. *rubra*) Ethanol Cream Extract of Dermic Collagen on Male Wistar Rats (*Rattus norvegicus*) Exposed to Ultraviolet B. *Intisari Sains Medis*, **11**(1); 253–258

Chauhan, I., M. Yasir, M. Verma, and A. P. Singh (2020). Nanostructured Lipid Carriers: A Groundbreaking Approach for Transdermal Drug Delivery. *Advanced Pharmaceutical Bulletin*, **10**(2); 150–165

Chou, H. Y., C. Lee, J. L. Pan, Z. H. Wen, S. H. Huang, C. W. J. Lan, W. T. Liu, T. C. Hour, Y. C. Hseu, B. H. Hwang, K. C. Cheng, and H. M. D. Wang (2016). Enriched Astaxanthin Extract from *Haematococcus pluvialis* Augments Growth Factor Secretions to Increase Cell Proliferation and Induces MMP1 Degradation to Enhance Collagen Production in Human Dermal Fibroblasts. *International Journal of Molecular Sciences*, **17**(6); 955

Davinelli, S., M. E. Nielsen, and G. Scapagnini (2018). Astaxanthin in Skin Health, Repair, and Disease: A Comprehensive Review. *Nutrients*, **10**(4); 522

Dewati, P. R., Rochmadi, A. Rohman, and A. Budiman (2022). Degradation Rate of Astaxanthin from *Haematococcus pluvialis*. *Food Research*, **6**(4); 254–258

Erawati, T., R. A. Arifiani, A. Miatmoko, D. M. Hariyadi, N. Rosita, and T. Purwanti (2023). The Effect of Peppermint Oil Addition on the Physical Stability, Irritability, and Penetration of Nanostructured Lipid Carrier Coenzyme Q10. *Journal of Public Health in Africa*, **14**(1); 2515

Erawati, T., D. M. Hariyadi, N. Rosita, and T. Purwanti (2021). Comparison of the Release Rate, Penetration and Physical Stability of p-Methoxycinamic Acid (PMCA) in Nanostructured Lipid Carriers (NLC), Solid Lipid Nanoparticle (SLN) and Nanoemulsion (NE) Systems. *Research Journal of Pharmacy and Technology*, **14**(11); 5719–5724

Geng, Q., Y. Zhao, L. Wang, L. Xu, X. Chen, and J. Han (2020). Development and Evaluation of Astaxanthin as Nanostructure Lipid Carriers in Topical Delivery. *AAPS PharmSciTech*, **21**(8); 1–12

Hariyadi, D. M., S. N. Sairiyah, F. W. Rahman, M. A. S. Rijal, N. Rosita, and M. Rahmadi (2024). Quercetin Solid Lipid Microparticle Stability and Deposition in Rat Lungs: A Study of Surfactant Effect. *Science and Technology Indonesia*, **9**(3); 682–696

Kang, W., D. Choi, and T. Park (2020). Decanal Protects Against UVB-Induced Photoaging in Human Dermal Fibroblasts via the cAMP Pathway. *Nutrients*, **12**(5); 1214

Khosa, A., S. Reddi, and R. N. Saha (2018). Nanostructured Lipid Carriers for Site-Specific Drug Delivery. *Biomedicine & Pharmacotherapy*, **103**; 598–613

Lambers, H., S. Piessens, A. Bloem, H. Pronk, and P. Finkel (2006). Natural Skin Surface pH Is on Average Below 5, Which Is Beneficial for Its Resident Flora. *International Journal of Cosmetic Science*, **28**(5); 359–370

Lee, H., Y. Hong, and M. Kim (2021). Structural and Functional Changes and Possible Molecular Mechanisms in Aged Skin. *International Journal of Molecular Sciences*, **22**(22); 12489

Lima, S. G. M., M. C. L. C. Freire, V. d. S. Oliveira, C. Solisio, A. Converti, and A. A. N. de Lima (2021). Astaxanthin Delivery Systems for Skin Application: A Review. *Marine Drugs*, **19**(9); 511

Mardiyanto, M., N. A. Fithri, A. Amriani, H. Herlina, and D. P. Sari (2021). Formulation and Characterization of Glibenclamide Solid Lipid Submicroparticles Formated by Virgin Coconut Oil and Solid Matrix Surfactant. *Science and Technology Indonesia*, **6**(2); 58–66

Miatmoko, A., N. A. Marufah, Q. Nada, N. Rosita, T. Erawati, J. Susanto, K. E. Purwantari, A. Nurkanto, Purwati, and W. Soeratri (2022). The Effect of Surfactant Type on Characteristics, Skin Penetration and Antiaging Effectiveness of Transfersomes Containing Amniotic Mesenchymal Stem Cells Metabolite Products in UV-Aging Induced Mice. *Drug Delivery*, **29**(1); 3443–3453

Nanic, L., A. Cedilak, N. S. Vidacek, F. Gruber, M. Huzak, M. Bader, and I. Rubelj (2022). In Vivo Skin Regeneration and Wound Healing Using Cell Micro-Transplantation. *Pharmaceutics*, **14**(9); 1955

Olejnik, A., J. Goscianska, and I. Nowak (2012). Active Compounds Release from Semisolid Dosage Forms. *Journal of Pharmaceutical Sciences*, **101**(11); 4032–4045

Patil, G. B., N. D. Patil, P. K. Deshmukh, P. O. Patil, and S. B. Bari (2016). Nanostructured Lipid Carriers as a Potential Vehicle for Carvedilol Delivery: Application of Factorial Design Approach. *Artificial Cells, Nanomedicine, and Biotechnology*, **44**(1); 12–19

Punu, G. F., Y. Harahap, Q. K. Anjani, P. Hartrianti, R. F. Donnelly, and D. Ramadon (2023). Solid Lipid Nanoparticles (SLN): Formulation and Fabrication. *Pharmaceutical Sciences and Research*, **10**(2); 55–66

Putranti, A. R., E. Hendradi, and R. Primaharinastiti (2017). Effectivity and Physicochemical Stability of Nanostructured Lipid Carrier Coenzyme Q10 in Different Ratio of Lipid Cetyl Palmitate and Alpha Tocopheryl Acetate as Carrier. *Asian Journal of Pharmaceutical and Clinical Research*, **10**(2); 146

Rodriguez-Ruiz, V., J. A. Salatti-Dorado, A. Barzegari, A. Nicolas-Boluda, A. Houaoui, C. Caballo, N. Caballero-Casero, D. Sicilia, J. B. Venegas, E. Pauthe, Y. Omidi, D. Letourneur, S. Rubio, V. Gueguen, and G. Pavon-Djavid (2018). Astaxanthin-Loaded Nanostructured Lipid Carriers for Preservation of Antioxidant Activity. *Molecules*, **23**(10); 2601

Souto, E. B., J. F. Fangueiro, A. R. Fernandes, A. Cano, E. Sanchez-Lopez, M. L. Garcia, P. Severino, M. O. Pa-

ganelli, M. V. Chaud, and A. M. Silva (2022). Physicochemical and Biopharmaceutical Aspects Influencing Skin Permeation and Role of SLN and NLC for Skin Drug Delivery. *Heliyon*, **8**(2); e08938

Tamjidi, F., M. Shahedi, J. Varshosaz, and A. Nasirpour (2014). Design and Characterization of Astaxanthin-Loaded Nanostructured Lipid Carriers. *Innovative Food Science and Emerging Technologies*, **26**; 366–374

Tichý, E., M. Žabka, K. Gardavská, A. Halenárová, Z. Kontšeková Scheerová, and M. Potúčková (2011). Dissolution and Spectrophotometric Determination of Astaxanthin in Aqueous Solutions. *Pharmazie*, **66**(8); 560–563

Zhang, S. and E. Duan (2018). Fighting Against Skin Aging: The Way from Bench to Bedside. *Cell Transplantation*, **27**(5); 729–738

